JOURNAL OF SYNCHROTRON RADIATION

ISSN 1600-5775

Diaboloidal mirrors: algebraic solution and surface shape approximations

Valeriy V. Yashchuk,* Kenneth A. Goldberg, Ian Lacey, Wayne R. McKinney, Manuel Sanchez del Rio and Howard A. Padmore

Advanced Light Source, Lawrence Berkeley National Laboratory, 1 Cyclotron Rd, Berkeley, CA 94720, USA. *Correspondence e-mail: vvyashchuk@lbl.gov

Received 10 February 2021
Accepted 7 May 2021

Edited by S. Svensson, Uppsala University, Sweden

Keywords: X-ray optics; diaboloidal mirror; analytical solution; shape approximation.

A new type of optical element that can focus a cylindrical wave to a point focus (or vice versa) is analytically described. Such waves are, for example, produced in a beamline where light is collimated in one direction and then doubly focused by a single optic. A classical example in X-ray optics is the collimated two-crystal monochromator, with toroidal mirror refocusing. The element here replaces the toroid, and in such a system provides completely aberration free, point-to-point imaging of rays from the on-axis source point. We present an analytic solution for the mirror shape in its laboratory coordinate system with zero slope at the centre, and approximate solutions, based on bending an oblique circular cone and a bent right circular cylinder, that may facilitate fabrication and metrology.

1. Introduction

The new generation of multi-bend achromat (MBA) lattice synchrotron sources now offers unprecedented X-ray brightness and coherence based on undulators. However, with narrow horizontal and vertical electron beam sizes, these sources also have extremely bright bending magnet sources. Due to the broadband nature of the light, bending magnet beamlines have application in a wide range of experiments from Laue micro-diffraction to protein crystallography.

The challenge with these sources is to produce an aberration-free image, even when accepting significant angular aperture. While in undulator beamlines we can have a series of orthogonal focusing mirrors due to the low angular aperture, accommodating the large angular fan in a bending magnet beamline requires the use of mirror elements with both sagittal and tangential focusing.

A classical example in X-ray optics is the bending magnet double-crystal monochromator, which uses a vertically collimating pre-mirror, a pair of parallel crystals, followed by a toroidal mirror. The toroidal mirror focuses from infinity in the vertical direction and from the real, diverging source in the horizontal direction, creating a point image. However, this astigmatic focusing scheme results in significant low order aberrations, including coma-like terms.

To minimize these aberrations, a toroidal mirror can be designed with a horizontal demagnification of 2:1, at which point it has been shown that the most significant low order aberration vanishes (MacDowell *et al.*, 2004). However, the aberrations are not eliminated, and they remain problematic for the small source sizes of new and upgraded storage rings. Thus, we need a new type of mirror, the 'diaboloid,' designed for perfect imaging.

A diaboloidal mirror (or 'diaboloid') is a reflecting surface that converts a spherical wave to a cylindrical wave (Fig. 1), or

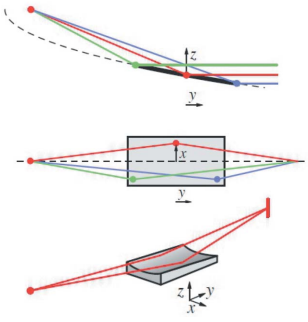

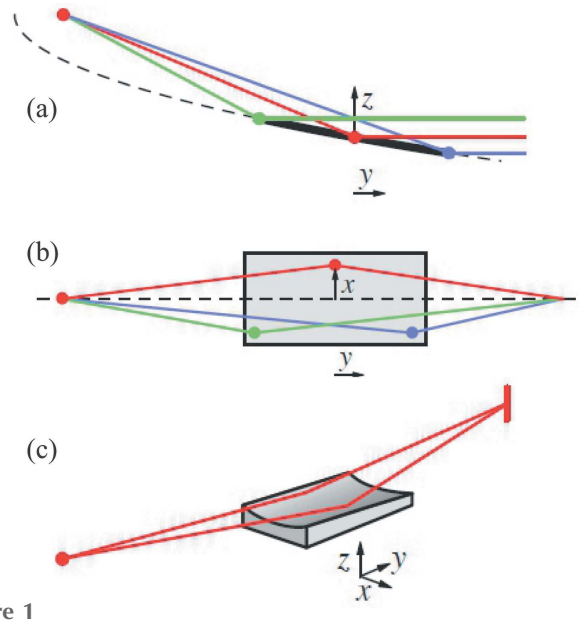

Figure 1
Three schematic views of the ray paths of the diaboloidal mirror illuminated from a point source (from the left) or from a one-dimensionally collimated source (from the right). (*a*) The side (vertical cross-section) view shows the parabolic cross-section, allowing a point source to be vertically collimated along the *y*-axis. (*b*) The top view shows sagittal focusing of diverging light. (*c*) A perspective view showing the point and sagittal line foci at conjugate positions. A mirror aperture-based (canonical) coordinate system (x, y, z) is depicted.

vice versa. The first derivation of the diaboloidal surface presented by McKinney *et al.* (2009) was carried out numerically using a polynomial series solution (up to sixth order) of the optical path problem. However, the polynomial approximation gives no insight into the underlying shape, and small changes in magnification require significant adjustment of the polynomial coefficients. Furthermore, describing the shape with the accuracy required by MBA sources requires expansion to even higher polynomial orders, where the mathematics becomes unwieldy.

The derivation of analytical expressions for the shape of a diaboloidal mirror in different coordinate systems, including the mirror-canonical and laboratory (mirror-related) coordinate systems (Fig. 2), was first described in a recent work (Yashchuk *et al.*, 2020).

The approach used by Yashchuk *et al.* (2020) is based on a representation of a diaboloidal mirror surface as a set of the cross-section segments of the ellipsoids of rotation focusing a point-source beam to certain points of the focal line interval (segment). This approach can be thought of as a 'purely geometrical' rather than classical geometrical optics that would be based on Fermat's principle. Nevertheless, in the course of the geometrical consideration, the condition of the equal optical path length for the focused rays arises 'automatically.'

In Yashchuk *et al.* (2020), the diaboloidal mirror shape equation $F(X, Y, Z) = 0$, defined in the mirror-related (rotated mirror-canonical) coordinate system (Fig. 2), is solved and coded in *Mathematica*™ in the form of a normal analytical

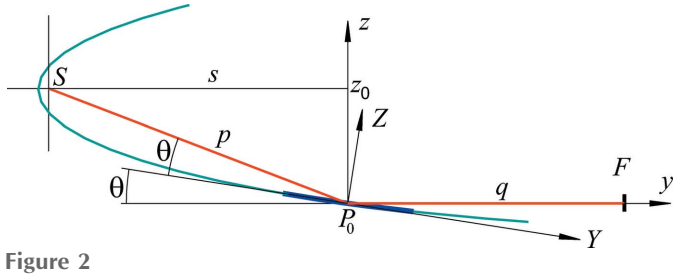

Figure 2
Schematic of the coordinate systems in use: the mirror-canonical coordinate system (x, y, z) (compare with Fig. 1) and the mirror-related coordinate system (X, Y, Z), where the tangent to the $X = 0$ profile at the mirror centre P_0 ($X = 0$, $Y = 0$, $Z = 0$) is equal to zero. The position of the source S is in the focal point of the diaboloid's generating parabola (the cyan line); F denotes the focus point for the central ray (the red lines). The conjugate (beamline optical design) parameters of the diaboloidal mirror (the thick blue line) are the object distance (from S to P_0), p, the image distance (from P_0 to F), q, and the angle of incidence for the central ray at the centre of the mirror, θ.

surface shape (profile) function $Z = f(X, Y)$ that describes the dependence of the mirror surface height Z on the position in the tangential Y and sagittal X coordinates. In spite of the fact that the exact analytical expression for $Z = f(X, Y)$, derived with the help of *Mathematica*™, is rather cumbersome, it allows numerical calculations of the desired diaboloidal three-dimensional surface profiles applicable, in particular, for ray-tracing simulations. However, the cumbersome appearance of the exact expression makes analysis difficult, for example, extracting allowable shape approximations.

Here, an exact analytical solution for the surface shape of a diaboloidal mirror as a function of the conjugate parameters of the mirror placed in a beamline is presented with a chain of algebraic transformations of the shape equation $F(X, Y, Z) = 0$ to the profile function $Z = f(X, Y)$. The resulting expressions are compact and convenient for straightforward coding in any software used for data processing and optical ray-tracing simulations. Based on the obtained analytical solution, we also derive the surface shapes approximating the diaboloid that can be easier for manufacturing with existing optical fabrication technologies. The analytical results of this paper are compared with the polynomial approximate solution (of the eighth order) of the optical path problem in McKinney *et al.* (2021) and are used in ray-tracing optical simulations discussed in detail by Sanchez del Rio *et al.* (2021).

2. Analytical expressions for the diaboloidal mirror shape

2.1. The mirror-canonical coordinate system

For completeness, we start from reproducing the surface shape equation of a diaboloidal mirror in the form $F(x, y, z) = 0$ presented by Yashchuk *et al.* (2020) but this time the derivations are explicitly based on the classical geometrical optics approach.

Following Fermat's principle, all path lengths from the object (point) to the image (line) must be of equivalent length K. We can express this as the sum of the distance from the

source to the mirror surface and the distance from the mirror to the focal line, following a path of constant z in the mirror-canonical coordinate system:

$$\left[x^2+(y+s)^2+(z_0-z)^2\right]^{1/2}+\left[x^2+(q-y)^2\right]^{1/2}=K. \quad (1)$$

The root of the quadratic equation (1) that corresponds to the diaboloidal mirror definition in Figs. 1 and 2 is

$$z=z_0-\left\{(K^2+q^2-s^2)-2(s+q)y -2K\left[x^2+(q-y)^2\right]^{1/2}\right\}^{1/2}. \quad (2)$$

By substituting into equation (2) the parameters K, s, and z_0 expressed via the conjugate parameters of the diaboloidal mirror (refer to Fig. 2):

$$K=p+q, \quad (3)$$

$$s=p\cos 2\theta, \quad (4)$$

$$z_0=p\sin 2\theta, \quad (5)$$

one can obtain the diaboloid shape equation in the mirror-canonical coordinate system [compare with the identical equation (16) in Yashchuk *et al.* (2020)]:

$$z=p\sin 2\theta-\left\{(p\sin 2\theta)^2+2q^2+2pq-2(p\cos 2\theta+q)y -2(p+q)\left[x^2+(q-y)^2\right]^{1/2}\right\}^{1/2}. \quad (6)$$

With $x=0$, equation (6) transforms to the expected parabolic profile along the tangential centre-line of the diaboloidal mirror:

$$z=p\sin 2\theta-2\sin\theta\left[p(y+p\cos^2\theta)\right]^{1/2}, \quad (7)$$

shown in Fig. 2 by the cyan line.

According to equation (6), the horizontal (z = constant) cross-sections of the diaboloidal mirror have elliptical shapes ensuring the mirror's property of sagittal focusing. This peculiarity of the diaboloidal mirror profile is exploited in Yashchuk *et al.* (2020) for the 'purely geometrical' derivation of the diaboloid shape equation identical to equation (6).

2.2. The mirror-related coordinate system

In order to express equation (6) as a function of the mirror-related coordinates X, Y, Z, we use the fact that the coordinate system (X, Y, Z) is rotated around the sagittal axis **X** (or, equivalently, **x**) by the angle of θ with respect to the coordinate system (x, y, z) and, therefore,

$$z=Z\cos\theta-Y\sin\theta, \quad (8)$$

$$y=Y\cos\theta+Z\sin\theta, \quad (9)$$

$$x=X. \quad (10)$$

Substitution of relations (8)–(10) into equation (6) leads to the diaboloidal mirror shape equation in the form [compare with the identical equation (18) in Yashchuk *et al.* (2020)]:

$$F(X,Y,Z)=-Z\cos\theta+Y\sin\theta+p\sin 2\theta -\left\{(p\sin 2\theta)^2+2q^2+2pq -2(p\cos 2\theta+q)(Y\cos\theta+Z\sin\theta) -2(p+q)\left[x^2+(q-Y\cos\theta-Z\sin\theta)^2\right]^{1/2}\right\}^{1/2} =0. \quad (11)$$

Below, we present an explicit solution of equation (11) as a chain of algebraic transformations that lead to the exact shape of a diaboloidal mirror in the form of a surface profile function $Z=f(X,Y)$. The solution is compact and convenient for applications.

3. Algebraic solution of the diaboloidal mirror shape equation

3.1. The idea of the solution

Having a combination of linear polynomials and a term with two square roots, enclosed one into the other and applied to second-order polynomial functions of the coordinates, equation (11) defines a surface described with a fourth-order polynomial function of coordinates X, Y, and Z. Therefore, upon straightforward algebraic manipulation, equation (11) can be transformed to an equation in the form of a quartic polynomial on the height variable Z [for classification of the polynomials see, for example, Degtyarev & Kharlamov (2000)]:

$$F_Q(X,Y,Z)=A(X,Y)Z^4+B(X,Y)Z^3+C(X,Y)Z^2+D(X,Y)Z+E(X,Y)=0, \quad (12)$$

where $B(X,Y)$, $C(X,Y)$, $D(X,Y)$, and $E(X,Y)$ are polynomial functions of X and Y of the first, second, third, and fourth order, respectively. In our case, the function $A(X,Y)$ is a constant coefficient of the fourth-order polynomial on Z and does not depend on X and/or Y.

Therefore, the first component of the derivation approach explored here is the determination of the diaboloid shape equation in the form of equation (12). When the diaboloid shape equation (12) is found, we apply to it the explicit radical solution of the quartic polynomial equation that was first derived in 1540 by Lodovico Ferrari and published in 1545. Now, the solution can be found in advanced handbooks and textbooks on algebra [see, for example, Korn & Korn (2000), van der Waerden (2001), and Stewart (2015)].

3.2. Diaboloidal mirror shape equation in the form of quartic polynomial

The first step of the algebraic manipulations is to equate the major square-root term in equation (11) to other terms and to square the result. Then, the obtained equation that contains a square-root term is regrouped to equate this square-root term

to the sum of the remaining terms. The result of this routine algebraic process is a comparatively simple equation:

$$\begin{aligned}-2(p+q)\left[X^2+(q-Y\cos\theta-Z\sin\theta)^2\right]^{1/2} &= \\ -2pq-2q^2+Y^2\sin^2\theta+2pY\cos\theta &\\ +2qY\cos\theta+Z^2\cos^2\theta-2pZ\sin\theta &\\ +2qZ\sin\theta-2YZ\sin\theta\cos\theta. &\end{aligned} \quad (13)$$

By squaring equation (13) and performing straightforward algebraic transformation to regroup the terms of the resulting equation according to the polynomial orders of the height variable Z, we obtain the diaboloidal mirror shape function in the form of quartic polynomial (12) with the coefficients:

$$A=-\cos^4\theta, \quad (14)$$

$$B(Y)=4(p-q)\cos^2\theta\sin\theta+4\cos^3\theta\sin\theta\,Y, \quad (15)$$

$$\begin{aligned}C(Y)=4q\left[(p+q)\cos^2\theta+4p\sin^2\theta\right] &\\ +2\cos\theta\left[q-3p+(p-3q)\cos 2\theta\right]Y &\\ -6\cos^2\theta\sin^2\theta\,Y^2, &\end{aligned} \quad (16)$$

$$\begin{aligned}D(Y)=-16pq(p+q)\sin\theta+4(p+q)(2p-q)\sin 2\theta\,Y &\\ +2\left[3p+q+(3q+p)\cos 2\theta\right]\sin\theta\,Y^2 &\\ +4\cos\theta\sin^3\theta\,Y^3, &\end{aligned} \quad (17)$$

$$\begin{aligned}E(X,Y)=4(p+q)^2X^2+4q(p+q)\sin^2\theta\,Y^2 &\\ -4(p+q)\cos\theta\sin^2\theta\,Y^3-\sin^4\theta\,Y^4. &\end{aligned} \quad (18)$$

Note that the zero-order coefficient $E(X, Y)$ is the only coefficient that depends on both spatial coordinates X and Y, while the first-, second-, and third-order coefficients depend only on the coordinate Y and the fourth-order coefficient is a constant.

3.3. Brief review of the explicit radical solution of the general quartic polynomial equation

The general quartic polynomial, usually analysed in the literature [see, for example, Korn & Korn (2000), van der Waerden (2001), and Stewart (2015)],

$$P_4(Z)=\tilde{a}Z^4+\tilde{b}Z^3+\tilde{c}Z^2+\tilde{d}Z^1+\tilde{e}=0, \quad (19)$$

can be simplified by dividing by $\tilde{a}$ in order to reduce the number of symbolic coefficients:

$$P_4(Z)=Z^4+bZ^3+cZ^2+dZ^1+e=0. \quad (20)$$

The four roots of the quartic polynomial equation (20) are:

$$Z1=-\frac{b}{4}-S+\frac{1}{2}\left(-4S^2-2k+\frac{m}{S}\right)^{1/2}, \quad (21)$$

$$Z2=-\frac{b}{4}-S-\frac{1}{2}\left(-4S^2-2k+\frac{m}{S}\right)^{1/2}, \quad (22)$$

$$Z3=-\frac{b}{4}+S+\frac{1}{2}\left(-4S^2-2k-\frac{m}{S}\right)^{1/2}, \quad (23)$$

$$Z4=-\frac{b}{4}+S-\frac{1}{2}\left(-4S^2-2k-\frac{m}{S}\right)^{1/2}, \quad (24)$$

where the coefficients k and m are

$$k=\left(8c-3b^2\right)/8, \quad (25)$$

$$m=\left(b^3-4bc+8d\right)/8, \quad (26)$$

and where S and Q are the coefficients given by the radical expressions:

$$S=\frac{1}{2}\left[\frac{1}{3}\left(Q+\frac{\Delta_0}{Q}\right)-\frac{2}{3}k\right]^{1/2}, \quad (27)$$

$$Q=2^{1/3}\left[\Delta_1+\left(\Delta_1^2-4\Delta_0^3\right)^{1/2}\right]^{1/3}, \quad (28)$$

with

$$\Delta_0=c^2-3bd+12e, \quad (29)$$

$$\Delta_1=2c^3-9bcd+27b^2e+27d^2-72ce. \quad (30)$$

The chain of equations (21)–(30) constitutes the explicit solution of the quartic polynomial equation (20) expressed by radicals. Here, we call this chain of equations the explicit radical solution.

3.4. Application of the explicit radical solution of the quartic polynomial equation to the diaboloidal shape equation

In this section, we combine the results of Sections 3.2 and 3.3 in order to establish a closed-loop chain of equations useful for calculation of the exact shape of a diaboloidal mirror. This can be done by expressing the coefficients b, c, d, and e in equation (20) via the coefficients A, B, C, D, and E of the quartic polynomial equation (12) for a diaboloidal mirror shape, derived in Section 3.2:

$$b=B/A, \quad c=C/A, \quad d=D/A, \quad e=E/A. \quad (31)$$

All these coefficients are the polynomial functions of the sagittal X and tangential Y coordinates in the mirror-related coordinate system of the diaboloidal mirror. The mirror conjugate parameters p, q, and θ are the parameters of these functions.

Next, we sequentially define the coefficients Δ_0 and Δ_1 with equations (29) and (30), k and m with equations (25) and (26), and S and Q with equations (27) and (28). Substitution of these coefficients as functions of b, c, d, and e, given by equation (31), into the formulas (21)–(24) for the roots of the quartic polynomial equation (20) provides the whole set of four solutions of the quartic polynomial equation for the diaboloidal shape. Among these four solutions, only the first one satisfies the conditions of $Z = 0$ at $X = Y = 0$. This solution provides the desired surface shape function of the diaboloidal mirror, defined with Fig. 2, as a dependence of the surface height Z on the coordinates X and Y:

$$Z(X,Y)=Z1=-\frac{b}{4}-S+\frac{1}{2}\left(-4S^2-2k+\frac{m}{S}\right)^{1/2}. \quad (32)$$

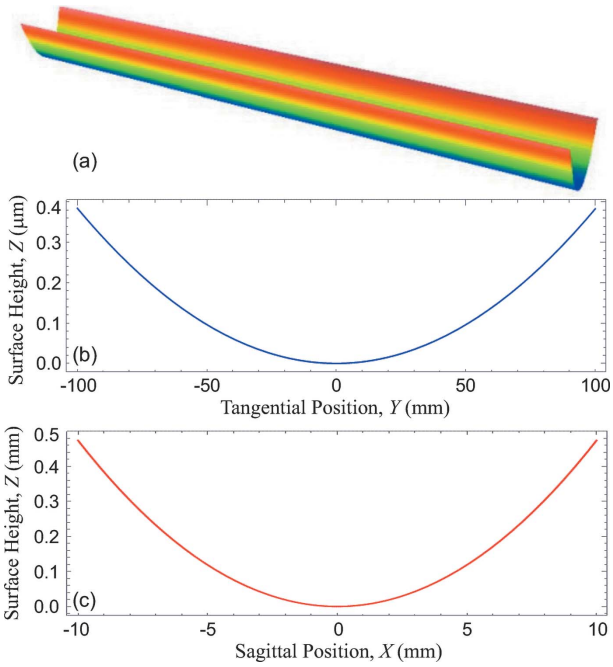

Figure 3
(*a*) Three-dimensional profile of a diaboloidal mirror, specified with the conjugate parameters given with equation (33). The mirror clear aperture with the tangential length of 200 mm and the sagittal width of 20 mm is depicted. (*b*, *c*) The surface height variations of the profile in plot (*a*) in the cross-sections $X = 0$ and $Y = 0$, respectively.

As an illustration, Fig. 3 depicts the shape of a diaboloidal mirror defined with the conjugate parameters

$$p = 29300.0 \text{ mm}, \quad q = 19530.0 \text{ mm}, \quad \theta = 0.0045 \text{ rad}. \tag{33}$$

The same parameters are used for the ray-tracing simulations in Yashchuk *et al.* (2020), where the diaboloid mirror profiles are numerically generated with a code in *Mathematica*™. Based on the analytical results presented here, the code has been upgraded to incorporate the explicit radical solution for the diaboloidal mirror shape in the mirror-related coordinate system. The code is designed to provide the diaboloidal mirror profiles in the format suitable for the *Shadow/Oasys* (Rebuffi & Sanchez del Rio, 2016) ray-tracing simulations described in Sanchez del Rio *et al.* (2021).

4. Diaboloid shape approximation with a sagittal circular cone bent to a tangential parabola

In this section, we analyse an approximation of the diaboloidal mirror shape with a sagittal circular cone bent to a tangential parabola. Such a shape is possibly easier to manufacture and to measure.

Note that in the simplified bending model discussed here, we ignore the second-order effects such as the anticlastic bending, which have to be taken into account in the course of the final-element-analysis treatment of a particular mirror design.

4.1. Circular cone best matching the sagittal profile of a diaboloidal mirror

In order to simplify the derivations, we use equation (6) for the diaboloidal mirror surface shape in the mirror-canonical coordinate system. First, we find analytical expressions for the cylindrical surface with the variation of the radius equal to the distribution of the diaboloid sagittal radius along its tangential axis. Then, the found solutions are transferred to the mirror-related coordinate system and the linear trend of the variation is used to define the desired circular cone. Finally, the bending of the circular cone is analytically modelled by adding a vertical offset to the circular cone's surface, corresponding to the diaboloid's generating parabola.

The dependence of the diaboloid's sagittal curvature on the tangential position at $x = 0$ is given by the second derivative of equation (6) [see, for example, Bronshtein *et al.* (2007)]. The corresponding expression for the radius of curvature valid for the mirror-canonical coordinate system is

$$R_{\rm C}(y) = \left[\frac{\partial^2 z(x,y)}{\partial x^2}\bigg|_{x=0}\right]^{-1} = \frac{2p(q-y)\,\sin\theta\,(y/p+\cos^2\theta)^{1/2}}{p+q}. \tag{34}$$

In the mirror-related coordinate system rotated by angle θ with respect to the mirror-canonical system (refer to Fig. 2), the vertical cross-sections of the cylindrical surface defined by the variation of the radius $R_{\rm C}(y)$, given with equation (34), have elliptical shape. Correspondingly, the sagittal radius at a certain tangential point along the mirror, calculated in the mirror-related coordinate system, is smaller by a factor of $\cos\theta$. We should also account for the effect of the rotation to the tangential position of the mirror surface point in the mirror-based coordinate system, $y = Y\cos\theta$. Accounting for these two factors in equation (34) leads to the following expression for the radius $R_{\rm M}(Y)$ of the cylindrical surface coincident with the diaboloid sagittal radius at $X = 0$ in the mirror-related coordinate system:

$$R_{\rm M}(Y) = \frac{2p(q-Y\cos\theta)\sin\theta\cos\theta\,(Y\cos\theta/p+\cos^2\theta)^{1/2}}{p+q}. \tag{35}$$

Figure 4 shows the lateral distribution of the radius of curvature defined with equation (35) at two different sets of the conjugate parameters.

In the vicinity of the mirror centre, $Y = 0$, the radius varies almost linearly in the case of Fig. 4(*a*), corresponding to the conjugate parameters given by equation (33), and stays approximately constant, if parameter p is changed to p = 9765.2 mm at the same values of parameters q and θ [Fig. 4(*b*)].

The second example is at the 2:1 horizontal demagnification condition, that previous work has shown to minimize aberrations and minimizes the height difference from the corresponding toroid. Below, we exploit the characteristic behaviour of $R_{\rm M}(Y)$ depicted in Fig. 4 to develop the approximations of the diaboloidal mirror with a bendable

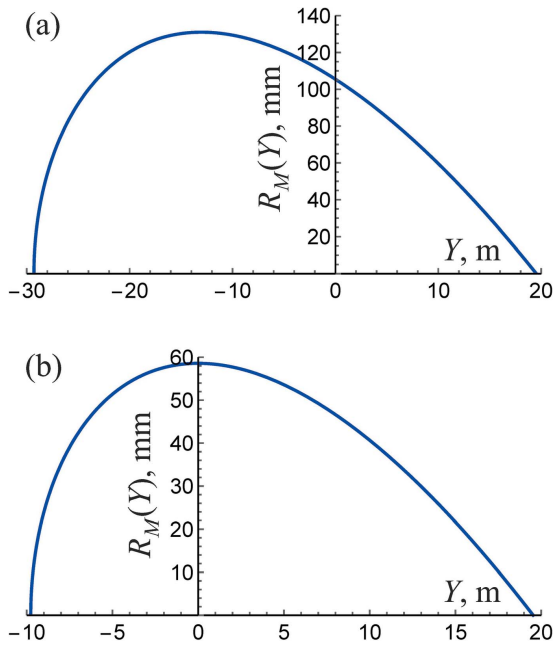

Figure 4
Distribution in the tangential direction of the sagittal radius of curvature $R_M(Y)$ defined with equation (35) at two different sets of the conjugate parameters: (*a*) p = 29300.0 mm, q = 19530.0 mm, and θ = 0.0045 rad, and (*b*) p = 9765.0 mm, q = 19530.0 mm, and θ = 0.0045 rad, corresponding to the 2:1 horizontal demagnification condition.

circular cone (this section) and a bendable right circular cylinder (Section 5).

In order to define the circular cone approximating the diaboloidal mirror, let us expand $R_M(Y)$ in a MacLaurin series of the normalized tangential variable $t = Y/p$. In most practical applications, the variable t is much smaller than one, $t \ll 1$. The first four terms of the series are:

$$R_M(t) \simeq R_{M0}\left(1 - \frac{2p\cos^2\theta - q}{2q\cos\theta}\,t - \frac{4p\cos^2\theta + q}{8q\cos^2\theta}\,t^2 + \frac{2p\cos^2\theta + q}{16q\cos^3\theta}\,t^3\right), \quad (36)$$

where

$$R_{M0} = \frac{2pq\cos^2\theta\sin\theta}{p+q} \quad (37)$$

is the diaboloid sagittal radius at the mirror centre, $X = Y = 0$. With the condition of $t \ll 1$, the variation of R_M is mostly determined by the linear term in the expansion (36), Fig. 5.

Figure 5(*a*) shows the variation of the sagittal radius $\delta R_M(Y) = R_M(Y) - R_{M0}$ of a 200 mm-long diaboloidal mirror defined with the conjugate parameters given by equation (33). In this case, at $Y = 0$, R_{M0} = 105.467 mm and the total variation is about ± 0.35 mm (peak-to-valley, PV). Note that the contribution to the variation $\delta R_{2,3,\ldots}(Y)$ of the polynomial terms in equation (36) of higher than the first order, depicted in Fig. 5(*b*), is smaller by almost three orders of magnitude than that of the linear term.

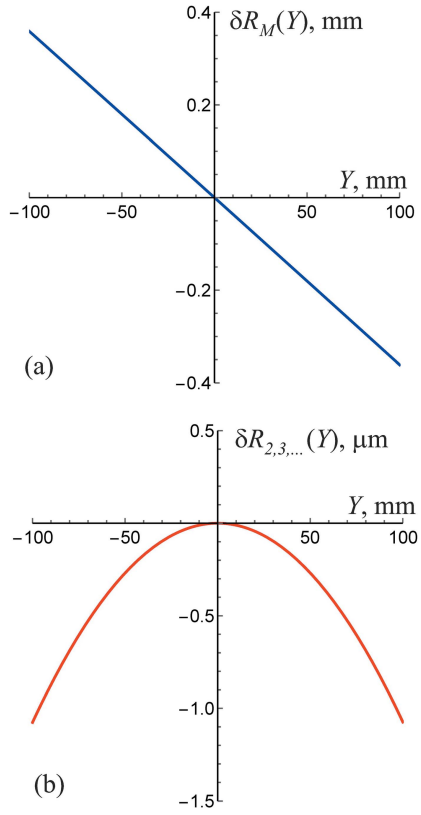

Figure 5
(*a*) Variation of the sagittal radius $\delta R_M(Y) = R_M(Y) - R_{M0}$ along the tangential direction of a 200 mm-long diaboloidal mirror defined by the conjugate parameters given by equation (33). (*b*) The contribution to the variation in plot (*a*) of the polynomial terms in equation (36) of higher than the first order, $\delta R_{2,3,\ldots}(Y)$.

Figure 6 illustrates the accuracy of the circular cone approximation in Fig. 5 in the sagittal height domain. At $Y = 0$ cross-section, the total variation of the sagittal height is about 0.5 mm (PV). The height error of the circular cone approximation, defined as a difference between the exact and approximation height traces, is less than 0.7 µm reaching the maximum at the sagittal edges of the mirror clear aperture at $X = \pm 10$ mm. Note that the sagittal height error, depicted in Fig. 6(*b*), scales as X^4. This immediately follows from the approximation of the sagittal share of the diaboloid (that is described with a function that is even with respect to the reversal of X, and odd orders are missing due to symmetry) with the circle.

In the circular cone approximation considered here, the tangential shape of the mirror is formed by mechanical bending of a pre-shaped circular cone substrate. Therefore, the approximation assumes that the substrate has no inherent height variation along the tangential direction at $X = 0$. Without loss of generality, we assume $H(X, Y) = 0$ at $X = 0$, where $H(X, Y)$ is the height of the substrate in the laboratory coordinate system. In order to satisfy this condition, each sagittal cross-section of the surface of the circular cone substrate, described with a canonical circle equation, has to be shifted in the vertical direction by the cylinder radius in the cross-section:

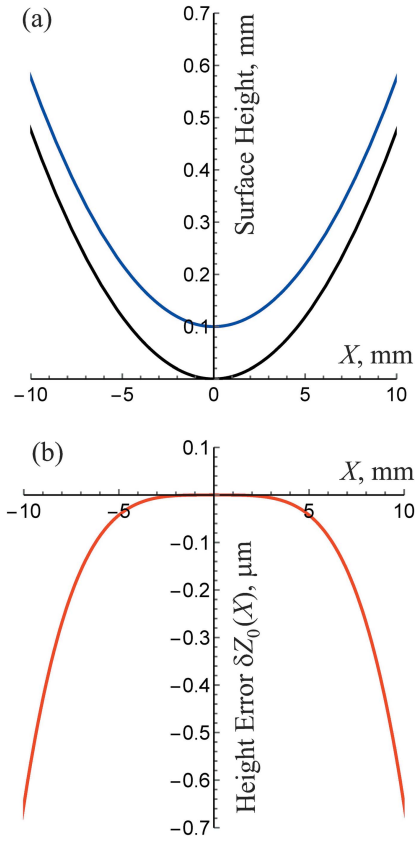

Figure 6
(*a*) Variation of the surface height in the sagittal direction at $Y = 0$ of the exact profile (the black line) and the conical approximation with the radius R_{M0}, given by equation (37) (the blue line) of the diaboloidal mirror defined by the conjugate parameters in equation (33). For clarity, the approximation trace is vertically shifted by 0.1 mm. (*b*) The height error of the conical approximation depicted as a difference between the exact and approximation height traces in plot (*a*). The difference is less than 1 μm across the range.

$$X^2 + \left[H(X, Y) + R_M(Y)\right]^2 = R_M^2(Y). \quad (38)$$

By substituting into equation (38) the linear approximation $R_1(Y)$ of the sagittal radius of the diaboloidal mirror, given with the first two terms of equation (36),

$$R_1(Y) = \frac{2pq\cos^2\theta\sin\theta}{p+q} - \frac{(2p\cos^2\theta - q)\cos\theta\sin\theta}{p+q}Y, \quad (39)$$

and transforming the circle equation (38) to the surface height function, one can describe the surface height profile of the substrate as an oblique circular cone:

$$H_1(X, Y) = R_1(Y) - \left[R_1^2(Y) - X^2\right]^{1/2}, \quad (40)$$

where the index '1' denotes that the oblique-circular-cone approximation accounts for only the linear polynomial in the MacLaurin series, equation (36). The signs in equation (40) correspond to the mirror arrangement depicted in Figs. 1 and 2 and treated throughout this paper.

4.2. Analytical model of bending an oblique circular cone

In order to analytically model the shape of the bent oblique circular cone (BOCC) $Z_{BOCC}(X, Y)$, the plane parabolic shape $P_M(X, Y)$, corresponding to the generating parabola of the diaboloidal mirror in the mirror-related coordinate system,

$$P_M(X, Y) = Y\tan\theta - 2\sec\theta\tan\theta\left(Yp\cos\theta + p^2\right)^{1/2} + 2p\sec\theta\tan\theta, \quad (41)$$

is added to the oblique-circular-cone surface $H_1(X, Y)$, given by equations (39) and (40):

$$Z_{BOCC}(X, Y) = H_1(X, Y) + P_M(X, Y). \quad (42)$$

Equation (41) is obtained from equation (7), derived for the mirror-canonical coordinate system, by accounting for the system's rotation with respect to the mirror-related coordinate system with equations (8) and (9).

Numerical treatment of the validity of the bent-oblique-circular-cone approximation (42) of the exact surface profile of a diaboloidal mirror is out of the scope of the present work. The corresponding ray-tracing simulations are discussed in detail by Sanchez del Rio *et al.* (2021).

5. Approximation of a diaboloidal mirror shape with a bent right circular cylinder

According to equation (36), if the mirror conjugate parameters obey the condition

$$q = 2p\cos^2\theta, \quad (43)$$

then the linear term in the MacLaurin series of the radius of the diaboloidal mirror curvature in the sagittal direction at $X = 0$ vanishes. This opens a possibility for design and fabrication of an approximation of a diaboloidal mirror with a bent right-circular-cylinder (BRCC) substrate. Condition (43) is the diaboloidal mirror equivalent to the condition of a '2:1 demagnification' that was first applied to the design of three protein crystallography beamlines at the Advanced Light Source (MacDowell *et al.*, 2004). It allows the optimization of the beamline performance of focusing toroidal mirrors by correcting the optical aberration (astigmatic coma) of the beamlines.

As an illustration, Fig. 7 depicts the shape of a diaboloidal mirror defined with the conjugate parameters

$$p = 9765.2 \text{ mm}, \quad q = 19530.0 \text{ mm}, \quad \theta = 0.0045 \text{ rad}, \quad (44)$$

where, compared with the conjugate parameters in equation (33), only parameter p is changed to satisfy the condition (43).

In this case shown in Fig. 4(*b*), the sagittal radius at $Y = 0$ is $R_{M0} = 58.5894$ mm and the total variation of the radius $\delta R_M(Y)$ along the tangential direction ($X = 0$) of the 200 mm-long diaboloidal mirror is only 2.3 μm with the second-order polynomial term dominating [Fig. 7(*a*)]. The deviation of the sagittal height of the BRCC approximation from the exact diaboloid profile is of the same level; at $Y = 0$, it reaches the maximum of about 2.1 μm at the sagittal edges of the clear aperture at $X = \pm 10$ mm [Fig. 7(*b*)].

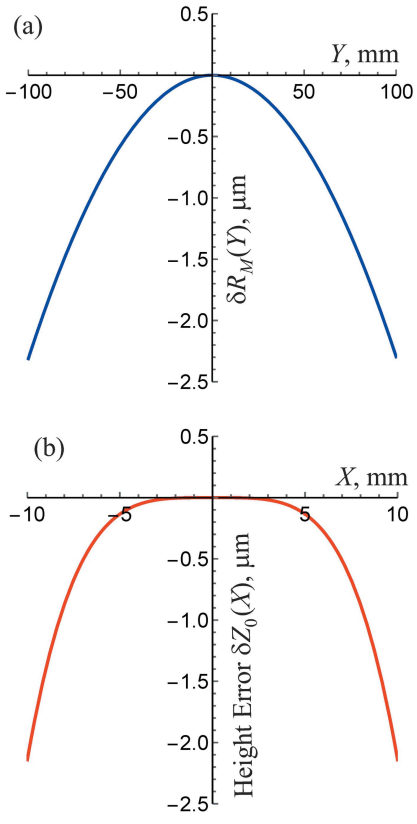

Figure 7
(*a*) Variation of the radius of the sagittal curvature $\delta R_{\rm M}(Y)$ along the tangential direction ($X = 0$) of a 200 mm-long diaboloidal mirror defined by the conjugate parameters given by equation (44). (*b*) The sagittal height error (at $Y = 0$) of the right-circular-cylinder approximation calculated as a difference between the exact-diaboloid trace and the approximation height trace with the radius $R_{\rm M0} = 58.5894$ mm.

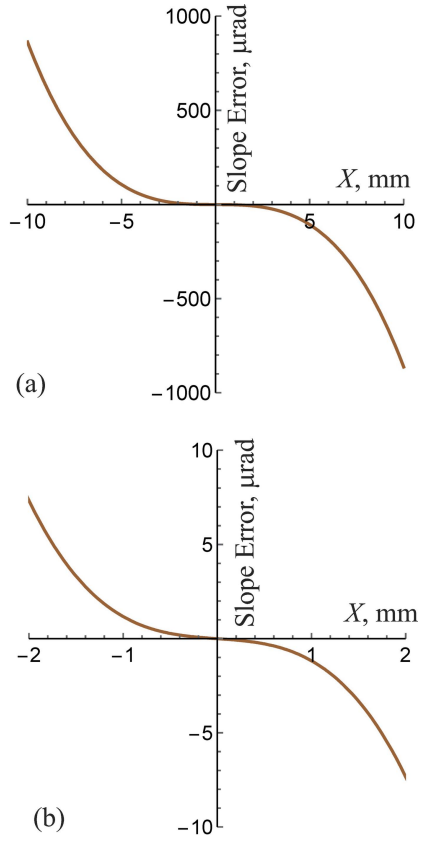

Figure 8
(*a*) The sagittal slope error (at $Y = 0$) of the right-circular-cylinder approximation to a diaboloidal mirror specified with the conjugate parameters (44). (*b*) The same as (*a*), but with the sagittal size of the mirror clear aperture reduced from ± 10 mm to ± 2 mm.

Similar to the BOCC approximation [Fig. 6(*b*)], the height error in the BRCC approximation is mainly described with the fourth-order polynomial term on the sagittal coordinate X. Therefore, at a sagittal clear aperture squeezed by a factor of five to ± 2 mm, the PV height error is only about 4 nm.

So far, we have analysed the approximation errors in the height domain. However, geometrical optics analysis and corresponding fabrication specification of X-ray optics are usually performed in the surface slope domain. In the content of the diaboloidal mirror approximation, the sagittal slope error is expected to be relatively large because of the much shorter sagittal size of a grazing-incidence mirror approximating a diaboloid.

In the case of the BRCC approximation under consideration here, the sagittal slope error in the mirror central cross-section ($Y = 0$) can be obtained by numerical differentiation of the height error trace shown in Fig. 7. The sagittal slope error trace obtained this way is presented in Fig. 8. At the sagittal edges of the mirror clear aperture ($X = \pm 10$ mm), the error reaches almost 900 μrad, Fig. 8(*a*). The error is relatively small only in the close vicinity of the mirror sagittal centre, Fig. 8(*b*).

Besides the significant shrinking of the sagittal size of the clear aperture, depicted in Fig. 8(*b*), the sagittal slope error can be additionally decreased by slightly adjusting the radius of the cylindrical surface. The adjustment of the radius $R_{\rm M0}$ by only +10 μm, from 58.5894 mm to 58.5994 mm, decreases the PV slope error from ± 7.5 μrad [Fig. 8(*b*)] to less than ± 2 μrad [Fig. 9(*a*)] at the same size of the clear aperture of ± 2 mm. For completeness, Fig. 9(*b*) shows the corresponding sagittal height error that is about 2 nm (PV).

The effect of the adjustment, depicted in Fig. 9(*a*), can be thought of as minimization of the slope variation in Fig. 8(*a*) by optimization of the cylindrical radius. A similar optimization is possible in the height domain if the figure of merit is the minimum of the height error.

Note that controlling in the course of fabrication, the sagittal radius of curvature of a right-circular-cylinder substrate with the accuracy on the level of 1 μm is a challenging problem. A more practical approach is the corresponding adjustment of the conjugate parameters of the mirror based on high-accuracy post-fabrication metrology [compare with equation (39)].

The result depicted in Fig. 9 validates the possibility of the high-accuracy right-circular-cylinder approximation (over a limited aperture) of a diaboloidal mirror designed for applications in a '2:1-magnification' arrangement. Obviously, a similar optimization of the radius $R_1(Y)$, given with equation (39), is applicable to the BOCC approximation of diaboloidal mirrors specified with the conjugate parameters disobeying

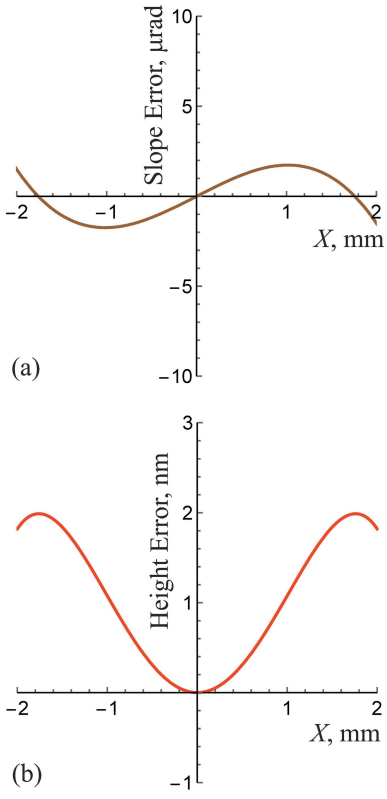

Figure 9
(*a*) The sagittal slope and (*b*) height errors (at $Y = 0$) of the right-circular-cylinder approximation to a diaboloidal mirror the same as in Fig. 8, but with the radius of the cylindrical surface R_{M0} adjusted by +10 μm, from 58.5894 mm to 58.5994 mm.

condition (43). A fine adjustment of the tangential parabolic shape upon bending can provide an additional possibility for the accurate compensation of the mirror astigmatic error.

Today's applications of the prospective exact diaboloidal mirrors and their possible approximations with bent right circular cylinders require mirrors with significantly improved surface quality and shape accuracy. In this respect, the BRCC approximation seems to be very attractive. First, the desired extraordinarily accurate right-circular-cylinder substrate can be fabricated with classical polishing technologies developed for manufacturing of X-ray sagittal cylinder mirrors and substrates for bendable toroidal mirrors. Second, the optical metrology instrumentation needed for surface characterization of the bendable toroidal mirrors have been developed at vendors' facilities for substrate fabrication and at optical metrology laboratories at X-ray light source facilities for tuning and characterization of bendable toroidal mirrors.

6. Summary

We have presented an *ab initio* chain of analytical expressions that describe the exact surface height topography of a diaboloidal mirror as a function of the conjugate parameters of the mirror's beamline application, distances from the mirror centre to the source and focus and the grazing-incidence angle.

The developed analytical description of the exact surface topography of a diaboloidal mirror has allowed us to approximate the diaboloidal shape with a sagittal oblique circular cone tangentially bent to match the diaboloid's generating parabola.

The established approximations and the described way for their further improvement via fine optimization of the sagittal radius potentially open a new avenue for development of bendable mirrors as a practical alternative to the exactly shaped diaboloidal mirrors for different beamline applications [for further discussion, see Sanchez del Rio *et al.* (2021)]. The found approximations provide a simple, calculational, and hence, relatively low-budget approach to the design and fabrication of bendable diaboloidal mirrors.

The most attractive approximation is a bent right-circular-cylinder diaboloidal mirror valid under the special '2:1 demagnification' condition, applied to the diaboloidal mirror conjugate parameters. In this case, the mirror sagittal cylinder substrate can be fabricated with conventional polishing techniques, used for fabrication of substrates for bendable toroidal mirrors. Moreover, the mid-spatial frequency surface-height deviation of a right-circular-cylinder substrate from the desired diaboloidal shape in the sagittal direction can possibly be corrected with application of one of the differential deposition/differential erosion techniques [see, for example, Kilaru *et al.* (2011), Windt & Conley (2015), Yokomae *et al.* (2018), Morawe *et al.* (2019), and references therein]. We are in the process of testing an additively corrected sagittal cylinder, using sputter deposition of platinum.

We should also mention that the recent advances in fabrication and metrology for three-dimensional aspherical optics [see, for example, Yamauchi *et al.* (2002), Wyant (2013), Nistea *et al.* (2019), and references therein] make diaboloidal mirrors feasible now.

The derived analytical expressions can be straightforwardly coded into software used for data processing and analysis, as well as for optical ray-tracing simulations. In our case, for numerical calculations of the desired diaboloid's three-dimensional surface profile we use a *Mathematica*™ code described in Yashchuk *et al.* (2020). The code, recently upgraded to incorporate the results of the present paper, is capable of the generation of diaboloidal mirror surface data applicable, in particular, for *Shadow/Oasys* (Rebuffi & Sanchez del Rio, 2016) ray-tracing simulations discussed in Sanchez del Rio *et al.* (2021). The *Shadow* simulations have confirmed the correctness of the derived analytical equations and their realization in the *Mathematica*™ and *Oasys* codes.

Acknowledgements

VVY dedicates this article to Viatcheslav Mikhailovich Kharlamov, Yury Josifovich Ionin, and Boris Mikhailovich Bekker, who were his mentors in advanced geometry and algebra essential for the derivations discussed in this article. The authors are very thankful to Alexander Givental and Viatcheslav Mikhailovich Kharlamov for useful discussions.

Funding information

The following funding is acknowledged: Director, Office of Science, Office of Basic Energy Sciences, Material Science Division, of the US Department of Energy (contract No. DE-AC02-05CH11231).

References

Bronshtein, L. N., Semindyayev, K. A., Musiol, G. & Muehlig, H. (2007). *Handbook of Mathematics*, 5th ed. Berlin: Springer.

Degtyarev, A. & Kharlamov, V. (2000). *Usp. Mater. Nauk.* **55**, 129–212; translation in Russian: *Math. Surveys*, **55**, 735–814.

Kilaru, K., Gregory, D. A., Ramsey, B. D. & Gubarev, M. V. (2011). *Opt. Eng.* **50**, 106501.

Korn, G. A. & Korn, T. M. (2000). *Mathematical Handbook for Scientists and Engineers*, 2nd ed. New York: Dover.

MacDowell, A. A., Celestre, R. S., Howells, M., McKinney, W., Krupnick, J., Cambie, D., Domning, E. E., Duarte, R. M., Kelez, N., Plate, D. W., Cork, C. W., Earnest, T. N., Dickert, J., Meigs, G., Ralston, C., Holton, J. M., Alber, T., Berger, J. M., Agard, D. A. & Padmore, H. A. (2004). *J. Synchrotron Rad.* **11**, 447–455.

McKinney, W. R. *et al.* (2021). *Theory of Diaboloidal Mirrors Applied to Protein Crystallography Beamlines.* In preparation.

McKinney, W. R., Glossinger, J. M., Padmore, H. A. & Howells, M. R. (2009). *Proc. SPIE*, **7448**, 744809.

Morawe, C., Labouré, S., Peffen, J.-C., Perrin, F., Vivo, A. & Barrett, R. (2019). *J. Synchrotron Rad.* **26**, 1872–1878.

Nistea, I.-T., Alcock, S. G., da Silva, M. B. & Sawhney, K. (2019). *Proc. SPIE*, **11109**, 1110906.

Rebuffi, L. & Sánchez del Río, M. (2016). *J. Synchrotron Rad.* **23**, 1357–1367.

Sanchez del Rio, M., Goldberg, K. A., Yashchuk, V. V., Lacey, I. & Padmore, H. A. (2021). *J. Synchrotron Rad.* **28**, 1041–1049.

Stewart, I. (2015). *Galois Theory*, 4th ed. New York: CRC Press.

Waerden, B. L. van der (2001). *Algebra*, Vol. 1, 7th ed., pp. 165–204. New York: Springer.

Windt, D. L. & Conley, R. Jr (2015). *Proc. SPIE*, **9603**, 96031H.

Wyant, J. C. (2013). *Appl. Opt.* **52**, 1–8.

Yamauchi, K., Mimura, H., Inagaki, K. & Mori, Y. (2002). *Rev. Sci. Instrum.* **73**, 4028–4033.

Yashchuk, V. V., Lacey, I. & Sanchez del Rio, M. (2020). *Proc. SPIE*, **11493**, 114930N.

Yokomae, S., Motoyama, H. & Mimura, H. (2018). *Precis. Eng.* **53**, 248–251.